

Improved Direct Torque Control for Single-phase Induction Motor Drives

THANATCHAI KULWORAWANICHPONG and TAWAT CHUCHIT

Power System Research Unit
 School of Electrical Engineering
 Suranaree University of Technology
 111 University Avenue, Nakhon Ratchasima
 THAILAND
 thanatchai@gmail.com

Abstract: - This paper illustrated a modified strategy of direct torque control for single-phase induction motors. The proposed strategy was based on classical six-sector hysteresis-type direct torque control scheme developed by using stator reference frame. The modification made in this paper led to two control strategies called modified six and twelve sectors, respectively. A switching table was derived based on the voltage vectors generated by the three-leg two-phase inverter topology. Simulations were carried out and performance analysis was presented.

Key-Words: - Single-phase induction motor drives, Direct torque control, Hysteresis control, Six-sector based DTC, Twelve-sector based DTC

1 Introduction

Three-phase induction motors have been increasingly important for industrial electric motor applications. It should note that there still exist DC motors in some limited applications, e.g. motors for vehicles. Apart from a large-size electric motor drive, single-phase induction motors are commonly used in household electric motor applications. These applications typically consume the power of a fractional horse power up to around ten horse powers. Although most electric appliances require a few amount of kilo-watt input, minimizing power losses during their operation gives a great benefit resulting in nationwide electric energy used by householders.

In general, single-phase motors are controlled by a thyristor-phase controller or a variable resistor. This is quite simple, but it is not efficient in terms of energy consumption. To achieve this goal, complex control strategy cannot be avoid as long as ac machines are involved. One of widely-used control schemes is variable-voltage, variable-frequency (VVVF) [1]. It can be applied for motor control in many forms. However, this control strategy does not guarantee minimum loss operation. Therefore, adjustable frequency and voltage of the power supply is more flexible and can lead to more economical operation of household electric appliances.

Over half a century, steady-state analysis of induction motors has become a powerful tool to characterize their performances [2-4]. It is fairly good in describing steady-state behaviors. For simple control where accuracy and precision are not that much important, any steady-state model is moderate. However, nowadays, a very accurate torque-speed control of induction motors via the space phasor theory, called vector control [5,6],

is increasingly required by industries [7,8]. However, there also exists some simple control technique that can give good performances in responses. One of them is Direct Torque Control (DTC). It gives outstanding features of fast torque response and simple control structure. In this paper, a modified DTC was proposed in order to enhance single-phase induction motor drive performances.

This paper describes six sections. Section 2 is a brief review of single-phase induction motor modeling using space phasor theory. Section 3 illustrates a basic DTC used as reference. Section 4 presents the modified DTC proposed in this paper. Results and discussion are in Section 5. The last section, Section 6, is conclusion.

2 Single-phase Induction Motor Model

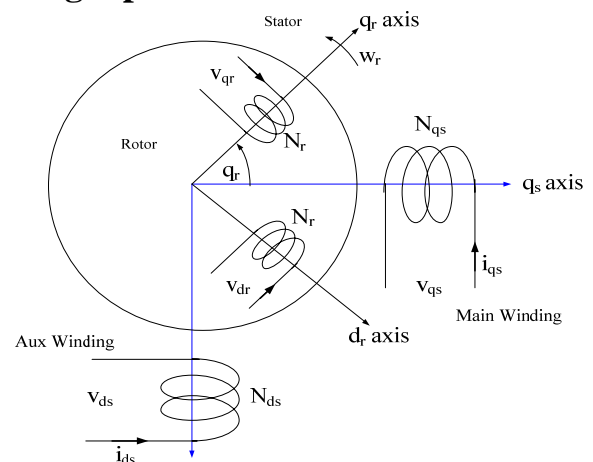


Fig. 1 Winding alignment of a single-phase motor

Single-phase induction motors can be characterized by several different models. The space-phasor approach [2,4] is the method used in this paper. With this model, motor currents, torque and speed can be observable. The space-phasor model is very complicated and needs more space for explanation. However, in this paper only a brief description is presented as follows.

Fig. 1 describes winding alignment of a single-phase induction motor consisting of main and auxiliary windings with their induced voltages and currents. As shown in the figure, a stationary reference frame which is along the axis of the main stator winding is defined and used for mathematical analysis throughout this paper. It is essential to inform that all quantities especially on the rotor need to be transferred to the stator axis. This can be performed by using the following transform matrix.

$$\begin{bmatrix} V_{qr}^s \\ V_{dr}^s \end{bmatrix} = \begin{bmatrix} \cos\theta_r & \sin\theta_r \\ -\sin\theta_r & \cos\theta_r \end{bmatrix} \begin{bmatrix} V_{qr}^r \\ V_{dr}^r \end{bmatrix} \quad (1)$$

The superscripts s and r indicate the reference axis in which the variable belongs to. The dynamic machine model for a single-phase induction motor with squirrel-cage rotor in a stationary reference can be expressed as follows [2].

$$\frac{d}{dt} \lambda_{qs} = -r_{qs} i_{qs} + v_{qs} \quad (2)$$

$$\frac{d}{dt} \lambda'_{ds} = -r'_{ds} i'_{ds} + v'_{ds} \quad (3)$$

$$\frac{d}{dt} \lambda_{qr}^{ts} = -r_r i_{qr}^{ts} + \omega_r \lambda'_{dr} \quad (4)$$

$$\frac{d}{dt} \lambda'_{dr} = -r_r i_{dr}^{ts} - \omega_r \lambda_{qr}^{ts} \quad (5)$$

By rearranging (2) – (5) based on flux linkage and current relations of the single-phase induction motor, the state-space model, in which stator and rotor currents, and rotor speed are state variables, can be formed.

$$\frac{d}{dt} [x] = [A][x] + [B][u] \quad (6)$$

$$[y] = [C][x] \quad (7)$$

Where

$$[x] = [i_{qs} \quad i'_{ds} \quad i_{qr}^{ts} \quad i_{dr}^{ts} \quad \omega_r]^T$$

$$[A] = [G]^{-1} [M]$$

$$[B] = [G]^{-1} [N]$$

$$[G] = \begin{bmatrix} L_{lqs} + L_{mq} & 0 & L_{mq} & 0 & 0 \\ 0 & L'_{lds} + L_{mq} & 0 & L_{mq} & 0 \\ L_{mq} & 0 & L'_{lr} + L_{mq} & 0 & 0 \\ 0 & L_{mq} & 0 & L'_{lr} + L_{mq} & 0 \\ 0 & 0 & 0 & 0 & 1 \end{bmatrix}$$

$$[M] = \begin{bmatrix} -r_{qs} & 0 & 0 & 0 & 0 \\ 0 & -r'_{ds} & 0 & 0 & 0 \\ 0 & X_m & -r_r & X_r & 0 \\ X_m & 0 & -X_r & -r_r & 0 \\ \alpha i_{dr}^{ts} & -\alpha i_{qr}^{ts} & 0 & 0 & -\frac{B_m}{J_m} \end{bmatrix}$$

$$[N] = \begin{bmatrix} 1 & 0 & 0 \\ 0 & 1 & 0 \\ 0 & 0 & 0 \\ 0 & 0 & 0 \\ 0 & 0 & -\frac{1}{J_m} \end{bmatrix}$$

$$X_m = \omega_r L_{mq}, X_r = \omega_r (L'_{lr} + L_{mq}), \alpha = \frac{P \cdot L_{mq}}{2J_m}$$

$i_{qs}, i'_{ds}, i_{qr}^{ts}, i_{dr}^{ts}, \lambda_{qs}, \lambda'_{ds}, \lambda_{qr}^{ts}, \lambda'_{dr}^{ts}$ are the current and flux linkage of the stator and rotor windings. $L_{lqs}, L'_{lds}, L'_{lr}$ are the leakage inductances of the stator and rotor windings. L_{mq} is the stator-rotor mutual inductance. r_{qs}, r'_{ds}, r_r are the stator and rotor resistances. All variables and parameters are referred to the stationary main-winding reference. J_m is motor's moment of inertia and B_m is damping coefficient.

Applying a numerical time-stepping method to solve a set of differential equations, motor currents, angular speed and position can be calculated numerically.

3 Direct Torque Control Schemes

A classical direct torque control [9] is given in Fig. 2. Inverters performed by following the command generated by using the control block diagram in Figure.

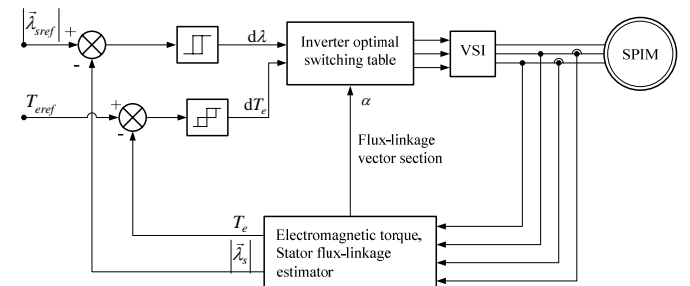


Fig. 2 Classical direct torque control

With this control strategy, stator flux and electromagnetic torque are both calculated by using the mathematical model given in the previous section. According to (2) and (3), stator flux linkages can be estimated by integrating these equations as expressed in (8) and (9). Eq. (10) gives the expression of torque estimation. Results from this calculation will be compared with flux and torque references. The errors are

interpreted by looking up a provided switching table for commanding the voltage source inverter [9-10].

$$\lambda_{qs} = \int (v_{qs} - r_{qs} i_{qs}) dt \quad (8)$$

$$\lambda'_{ds} = \int (v'_{ds} - r'_{ds} i'_{ds}) dt \quad (9)$$

$$T_e = \frac{P}{2} (i_{qs} \lambda'_{ds} - i'_{ds} \lambda_{qs}) \quad (10)$$

For single-phase inverter-fed induction motors, a classical space vector technique similar to that of three-phase inverter-fed induction motors. It consists of six unsymmetrical non-zero vectors and two zero vectors as shown in Fig. 3.

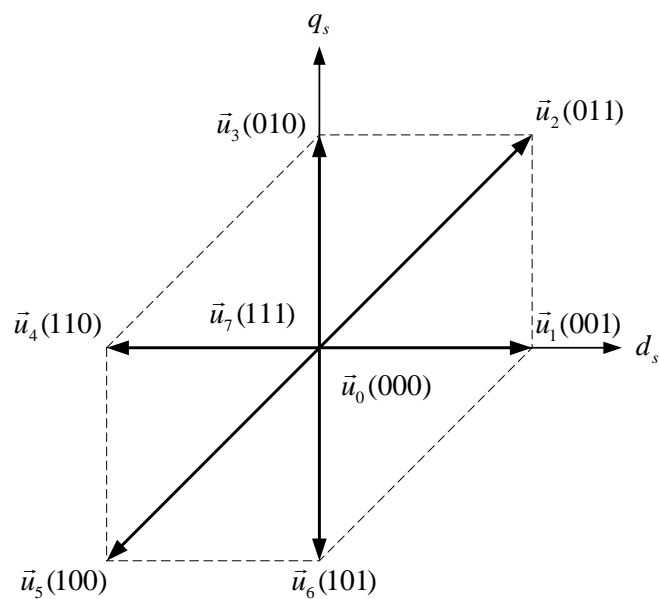


Fig. 3 Space vector for inverter control

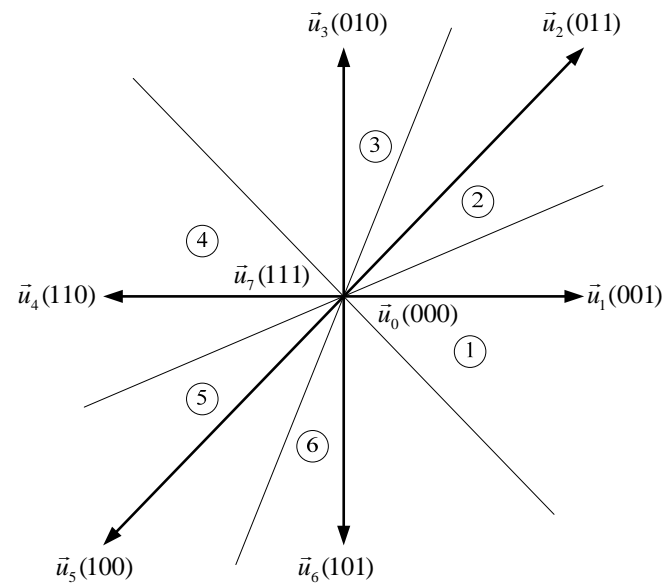


Fig. 4 Basic six-sector based DTC

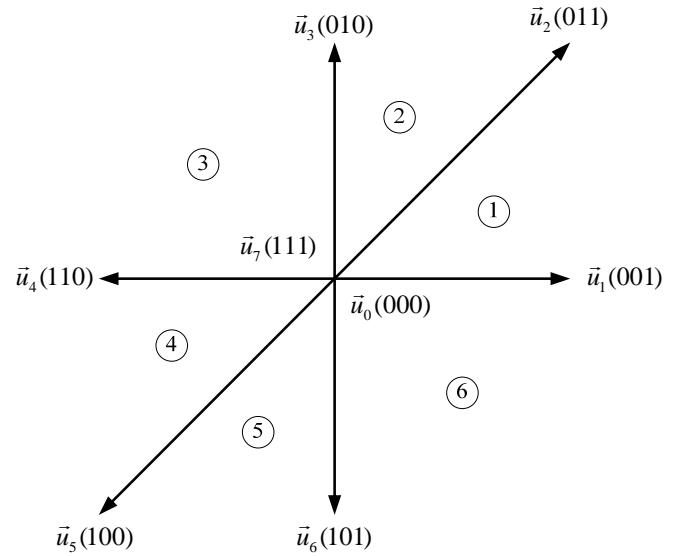


Fig. 5 Modified six-sector based DTC

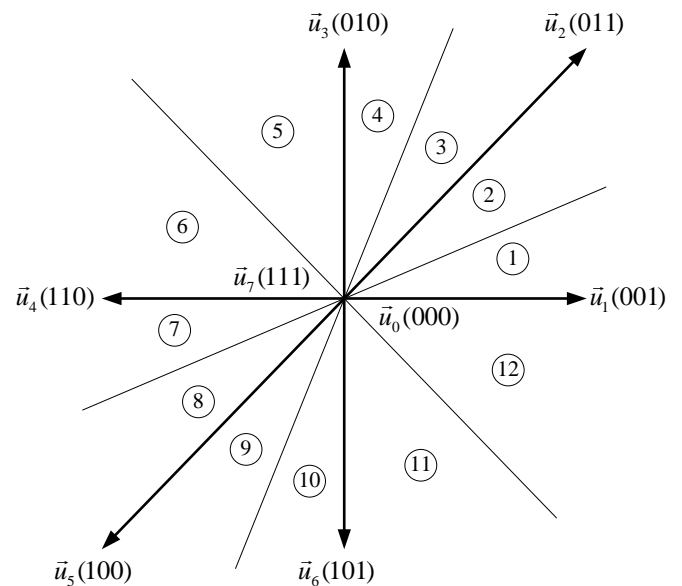


Fig. 6 Modified six-sector based DTC

Neglecting the stator resistance, stator flux can be simplified by (11). This implies that the change of stator flux is proportional to voltage applied to the stator circuit [11-12]. Basically, switching commands of VSI can be divided into six sectors as shown in Fig. 4. Also, the switching commands can be summarized in Table 1. Due to asymmetrical vectors, it is possible to rearrange six sectors to other locations. This modification gives a new control strategy of six-sector based DTC and better responses can be achieved. The relocation of six sectors is presented in Fig. 5 and the switching commands are summarized in Table 2.

As can be seen, accurate control of DTC can be improved by using more sectors. In this paper, twelve-sector based DTC is demonstrated. Fig. 6 shows the

overview of the twelve-sector operation. Its commands are summarized in Table 3.

Table 1 Switching table for classical DTC

$d\lambda$	dT_e	sector					
		1	2	3	4	5	6
1	1	\vec{u}_2	\vec{u}_3	\vec{u}_4	\vec{u}_5	\vec{u}_6	\vec{u}_1
	0	\vec{u}_0	\vec{u}_0	\vec{u}_7	\vec{u}_7	\vec{u}_7	\vec{u}_0
	-1	\vec{u}_6	\vec{u}_1	\vec{u}_2	\vec{u}_3	\vec{u}_4	\vec{u}_5
0	1	\vec{u}_3	\vec{u}_4	\vec{u}_5	\vec{u}_6	\vec{u}_1	\vec{u}_2
	0	\vec{u}_7	\vec{u}_7	\vec{u}_0	\vec{u}_0	\vec{u}_0	\vec{u}_7
	-1	\vec{u}_5	\vec{u}_6	\vec{u}_1	\vec{u}_2	\vec{u}_3	\vec{u}_4

Table 2 Switching table for modification of six-sector based DTC

$d\lambda$	dT_e	sector					
		1	2	3	4	5	6
1	1	\vec{u}_3	\vec{u}_3	\vec{u}_4	\vec{u}_6	\vec{u}_6	\vec{u}_1
	0	\vec{u}_0	\vec{u}_0	\vec{u}_7	\vec{u}_7	\vec{u}_7	\vec{u}_0
	-1	\vec{u}_1	\vec{u}_1	\vec{u}_2	\vec{u}_4	\vec{u}_4	\vec{u}_5
0	1	\vec{u}_4	\vec{u}_4	\vec{u}_5	\vec{u}_1	\vec{u}_1	\vec{u}_2
	0	\vec{u}_7	\vec{u}_7	\vec{u}_0	\vec{u}_0	\vec{u}_0	\vec{u}_7
	-1	\vec{u}_6	\vec{u}_6	\vec{u}_1	\vec{u}_3	\vec{u}_3	\vec{u}_4

Table 3 Switching table for twelve-sector DTC

$d\lambda$	dT_e	sector					
		1	2	3	4	5	6
1	1	\vec{u}_3	\vec{u}_3	\vec{u}_4	\vec{u}_4	\vec{u}_6	\vec{u}_6
	0	\vec{u}_0	\vec{u}_0	\vec{u}_7	\vec{u}_7	\vec{u}_0	\vec{u}_0
	-1	\vec{u}_1	\vec{u}_1	\vec{u}_2	\vec{u}_2	\vec{u}_4	\vec{u}_4
0	1	\vec{u}_4	\vec{u}_4	\vec{u}_5	\vec{u}_5	\vec{u}_1	\vec{u}_1
	0	\vec{u}_7	\vec{u}_7	\vec{u}_0	\vec{u}_0	\vec{u}_7	\vec{u}_7
	-1	\vec{u}_6	\vec{u}_6	\vec{u}_1	\vec{u}_1	\vec{u}_3	\vec{u}_3
$d\lambda$	dT_e	sector					
1	1	\vec{u}_6	\vec{u}_6	\vec{u}_1	\vec{u}_1	\vec{u}_3	\vec{u}_3
	0	\vec{u}_0	\vec{u}_0	\vec{u}_0	\vec{u}_0	\vec{u}_0	\vec{u}_0
	-1	\vec{u}_4	\vec{u}_4	\vec{u}_5	\vec{u}_5	\vec{u}_1	\vec{u}_1
0	1	\vec{u}_1	\vec{u}_1	\vec{u}_2	\vec{u}_2	\vec{u}_4	\vec{u}_4
	0	\vec{u}_7	\vec{u}_7	\vec{u}_7	\vec{u}_7	\vec{u}_7	\vec{u}_7
	-1	\vec{u}_3	\vec{u}_3	\vec{u}_4	\vec{u}_4	\vec{u}_6	\vec{u}_6

4 Simulation Results

To verify the effectiveness of the proposed DTC, stator flux was assumed to be regulated at 0.8 Wb while electromagnetic torque was controlled as follows.

$$T_{eref} = 0.0 \text{ N.m} \quad \text{for } 0 \text{ s} \leq t \leq 0.5 \text{ s}$$

$$T_{eref} = 2.0 \text{ N.m} \quad \text{for } 0.5 \text{ s} \leq t \leq 2.0 \text{ s}$$

$$T_{eref} = -2.0 \text{ N.m} \quad \text{for } 2.0 \text{ s} \leq t \leq 2.25 \text{ s}$$

$$T_{eref} = 1.0 \text{ N.m} \quad \text{for } 2.25 \text{ s} \leq t \leq 3.0 \text{ s}$$

By applying three different schemes of DTC for single-phase induction motor drives with hysteresis control of a specified error band, results of current, torque and flux responses can be shown in Fig. 7, 8 and 9 for the classical DTC, modified six-sector DTC and twelve-sector DTC, respectively.

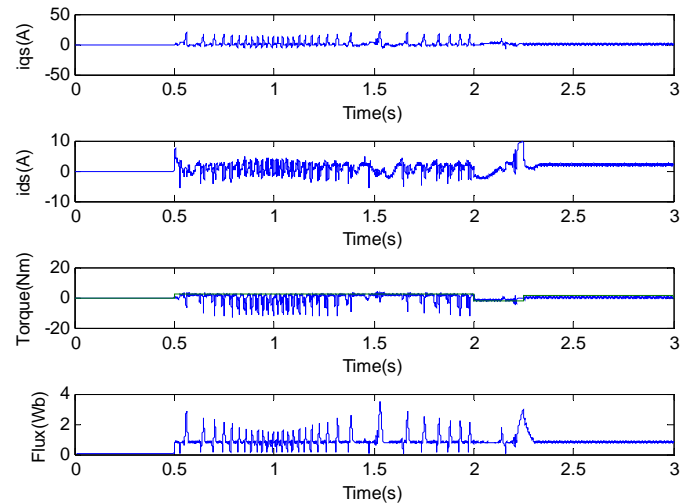


Fig. 7 Responses of the classical DTC case

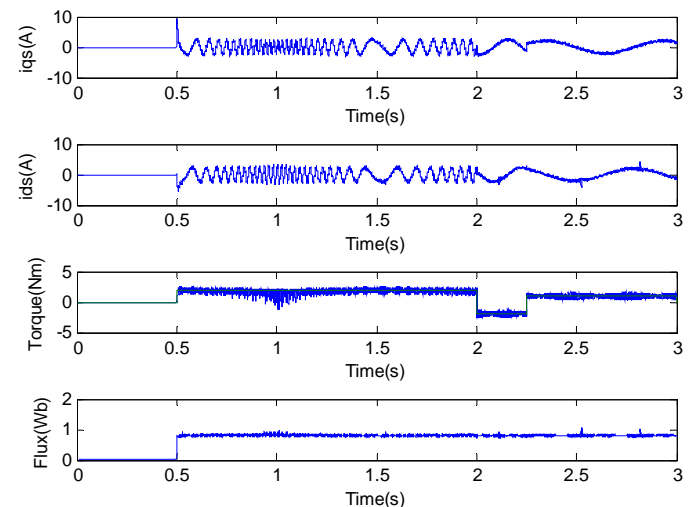


Fig. 8 Responses of the modified six-sector DTC case

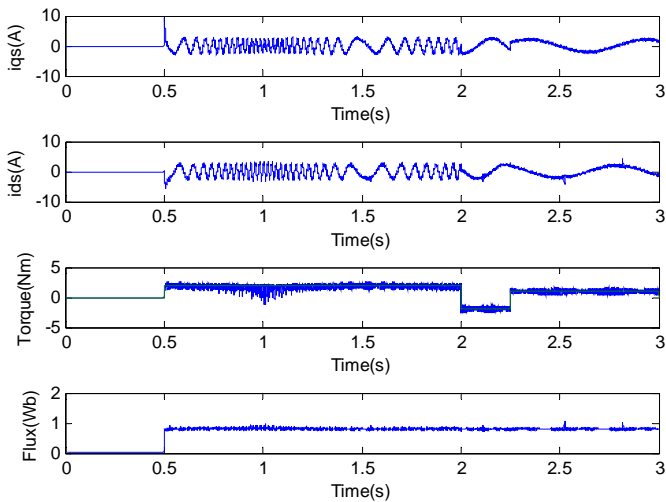


Fig. 9 Responses of the twelve-sector DTC case

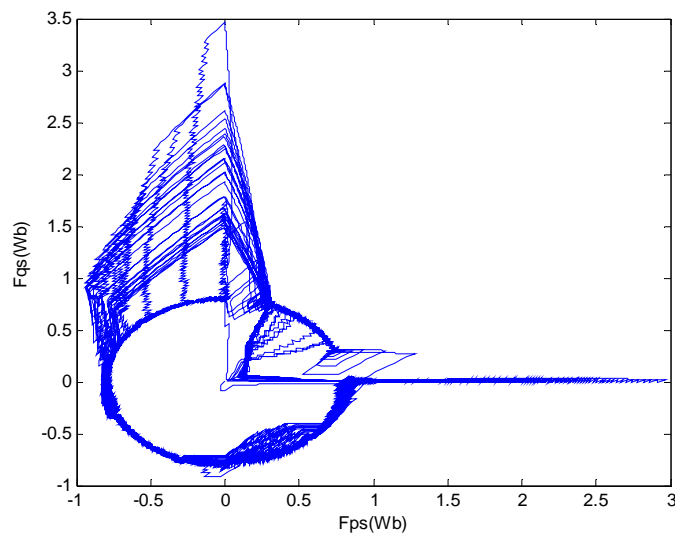


Fig. 10 Stator flux of the classical DTC case

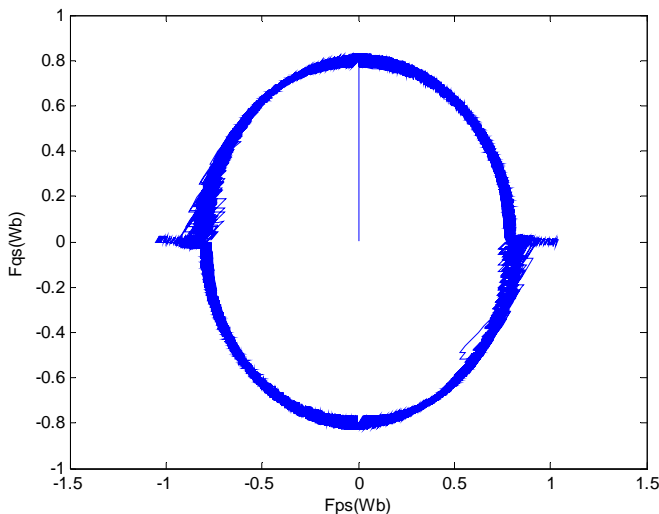


Fig. 11 Stator flux of the modified six-sector DTC case

As can be seen, the results showed that two proposed DTC schemes can be used to regulate both flux and torque more accurate than those controlled by the

classical DTC. This can be explained by visualizing stator flux trajectory of the motor due to the operation for all three cases as shown in Figs 10 – 12.

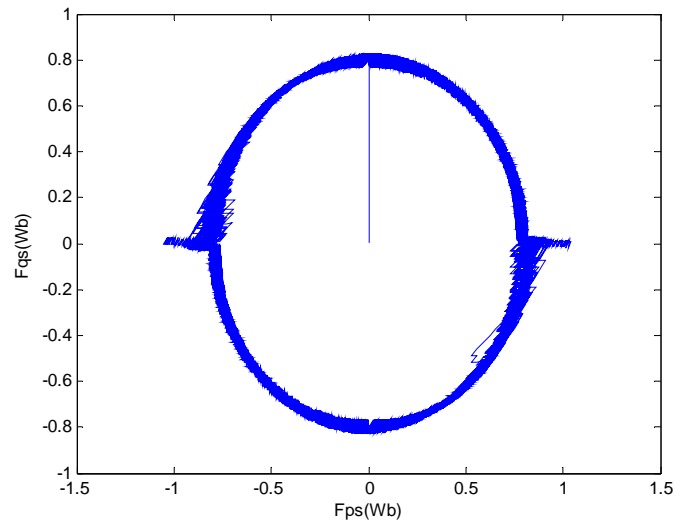


Fig. 12 Stator flux of the twelve-sector DTC case

5 Conclusion

This paper presented a modified six-sector based DTC and a twelve-sector based DTC for single-phase induction motor drives. Looking-up table based switching control of the inverter was provided. Test was conducted to perform the stator flux and torque regulation. As a result, the modified six-sector based DTC and the proposed twelve-sector based DTC gave satisfactory results and this confirmed the effectiveness of the proposed DTC schemes.

6 Acknowledgment

The authors would like to acknowledge the financial support of the research grant sponsored by the National Research Committee of Thailand (NRCT), during a period of this work.

References:

- [1] P.C. Krause, *Analysis of Electric Machines*, McGraw-Hill, 1987.
- [2] N. Naewngerndee, C. Sukcharoen, T. Kulworawanichpong, "Simulation of Single-Phase Induction Motor Drives with Non-sinusoidal Power Supply". *The WSEAS Transactions on Systems*, Issue 5, Vol 5, pp. 1029-1034, 2006
- [3] R. Krishnan, *Electric motor drives – modelling, analysis and control*, Prentice-Hall, 2001
- [4] S. Raweekul, T. Kulworawanichpong, S. Sujitjorn, "Parallel -Connected Single -Phase Induction Motor:Modelling and Simulation", *The WSEAS*

Transactions on Circuits and Systems, Issue 3, Vol 5, pp. 377-384

- [5] J.W.L. Nerys, A. Hughes & J. Corda, Alternative implementation of vector control for induction motor and its experimental evaluation, *IEE Proceedings-Electric Power Applications*, 147(1), 2000, pp. 7–13.
- [6] M. Yano & M. Iwahori, Transition from slip-frequency control to vector control for induction motor drives of traction applications in Japan, *The 5th International Conference on Power Electronics and Drive Systems*, 2003, Saitama, Japan, pp. 1246–1251.
- [7] S. Shinnaka, S. Takeuchi, A. Kitajima, F. Eguchi & H. Haruki, Frequency-hybrid vector control for sensorless induction motor and its application to electric vehicle drive, *IEEE 16th Annual Applied Power Electronics Conference and Exposition, 2001*, Yokohama, Japan, pp. 32–39.
- [8] M. Benhaddadi, K. Yazid & P. Khaldi, An effective identification of rotor resistance for induction motor vector control, *Proc. IEEE Instru. and Meas. Tech. Conf.*, 1997, Ottawa, Canada, pp. 339–342.
- [9] P. Vas, *Sensorless Vector and Direct Torque Control*, Oxford University Press, 1998.
- [10] Y.V.Siva Reddy, M.Vijayakumar and T. Brahmananda Reddy, Direct Torque Control of Induction Motor Using Sophisticated Lookup Tables Based on Neural Networks, *AIML Journal*, June 2007.
- [11] F.A.S. Neves, E.B.S. Filho, J.M.S. Cruz, R.P. Landim, Z.D. Lins, A.G.H. Accioly, Single-phase induction motor drives with direct torque control, *The 28th Annual Conference on IEEE Industrial Electronics Society (IECON02)*, 2002.
- [12] R. de F. Campos, L.F.R. Pinto, J.de Oliveira, A.Nied, L.C.de Marques, A.H.de Souza, Single-Phase Induction Motor Control Based on DTC Strategies, *IEEE International Symposium on Industrial Electronics (ISIE 2007)*, 4-7 June 2007.